Modulation of Hydrophobic Effect by Cosolutes

Alessandro Di Michele,[†] Mariangela Freda,[†] Giuseppe Onori,[†,§] Marco Paolantoni,[‡] Aldo Santucci,*[,†] and Paola Sassi[‡]

Dipartimento di Fisica, Università di Perugia, CEMIN (Centro di Eccellenza Materiali Innovativi Nanostrutturati per Applicazioni Chimiche, Fisiche e Biomediche) I-06100 Perugia, Italy, Dipartimento di Chimica, Università di Perugia, I-06100 Perugia, Italy, and INFM-CRS SOFT, Unità di Perugia

Received: April 25, 2006

This work concerns a comparison of the hydration properties and self-association behavior in aqueous solution of three biologically relevant simple molecules: *tert*-butyl alcohol (TBA), trimethylamine-*n*-oxide (TMAO), and glycine betaine (GB). These molecules were used as a model to study hydrophobic behavior in water solutions. In particular, water perturbation induced by TBA, TMAO, and GB molecules was studied as a function of the solute molar fraction X_2 ($0 < X_2 < 0.04$) by Raman spectra of water in the fundamental OH-stretching region (3800−2800 cm^{-1}). Furthermore, possible hydrophobic clustering of these molecules was investigated by studying the behavior of the alkyl CH stretching band in the 3100−2900 cm^{-1} frequency region as a function of X_2. To establish the existence of a correlation between the effects of these three solutes on the micellization process and changes in the properties of the solvent, the behavior of the critical micelle concentration of sodium dodecyl sulfate was also investigated as a function of the added amount of TBA, TMAO, and GB. On the whole, these data show that there is no direct correlation between a solute's effect on the water structure and its effect on micelle or protein stability. Results indicate that, while TBA starts to self-aggregate at approximately $X_2 = 0.025$, both TMAO and GB do not exhibit any significant self-aggregation up to the highest concentration considered. In addition, nonadditive perturbations of the H-bonded networks of solvent water are observed in the case of TBA solutions, but are absent in both the TMAO and GB cases. The absence of these nonlinear effects in TMAO and GB water solutions allow for tracing the microscopical mechanism of the neutrality of these osmolytes toward hydrophobic effects. This confers the compatibility to these two osmolytes, which can be accumulated at high concentrations without interfering with biochemical processes in the cell.

Introduction

In recent years, the interest in the study of hydrophobic effects has noticeably increased in connection with the important role these effects play in protein folding, micelle formation, and in the stability of biological membranes. Hydrophobic effects arise from basic interactions between hydrophobic species and water molecules (hydrophobic hydration) as well as from the solvent-mediated interactions among hydrophobic groups (hydrophobic interactions). Despite the large amount of studies on this subject, there remains considerable debate about the molecular origin of hydrophobic effects.[1−3] Such effects arise from the unique three-dimensional structure of water and should be changed considerably by variation in the solvent structure due to change in temperature or the addition of cosolvents. A common method of investigating the role played by the solvent in maintaining the protein's native state involves the study of the conformation and thermal stability of these macromolecules in altered water structures by adding small quantities of monohydric alcohols of varying chain length.[4] This same approach is widely used to modify the rate and yield of many chemical reactions[5] and to influence the formation of micelles and biological membranes as well.[6] Actually, the mechanism of the action of alcohols on biomolecules is still obscure, and there are different views as to whether this action can be regarded as ligand binding or indirect, involving changes in the solvent properties. Examination of the literature reveals that the effects of alcohol−water mixtures on the conformation of proteins are indeed very complex, and lowering the dielectric constant of the solvent is not enough to explain such effects.[4,7] Whereas the general effect of alcohols is to destabilize the native state, at low concentrations, they promote a more ordered or more tightly folded conformation. The protein conformation appears to be stabilized or destabilized not just by neighbor interactions, but rather more subtle effects play a crucial role.

In previous studies related to the properties of alcohol/water mixtures, we have shown the occurrence of some kind of hydrophobic clustering of alcohol molecules in the water-rich region of compositions beyond a threshold alcohol concentration, X_2^*.[7] In all cases, mixture properties such as the molar volume, compressibility, and IR absorption show an anomalous behavior, which occurs in the water-rich region of compositions and which, for each alcohol, singles out the critical solvent concentration X_2^*. The observed behavior suggests that, for $X_2 < X_2^*$, the alcohol molecules are essentially dispersed and surrounded by "water cages" where the short-range order and microdynamics of the water molecules are changed with respect to those of pure water. Alcohol molecules are in mutual contact

* Corresponding author. Address: Dipartimento di Fisica, Università di Perugia, Via A. Pascoli, I-06100 Perugia, Italy. E-mail: papersbio@fisica.unipg.it.
† Dipartimento di Fisica, Università di Perugia.
‡ Dipartimento di Chimica, Università di Perugia.
§ INFM-CRS SOFT.

10.1021/jp068055w CCC: $33.50
Published on Web 10/04/2006

only at higher concentrations, when almost all the water molecules are involved in hydration shells of the alcohol molecules. Our studies indicate that the global mixing scheme of water−alcohol mixtures, including the possibility of cosolvent clustering effects, can have a dramatic influence on the conformation and stability of biomolecules and on the micellization process.[7]

Within the class of water-soluble monohydric alcohols, the *tert*-butyl alcohol (TBA) is the molecule with the largest hydrophobic group; that is, it is the most hydrophobic molecule among the low-weight water-soluble alcohols. In recent works, the hydration properties and the self-aggregation behavior of TBA in water have been compared with those of aqueous solutions of a biologically relevant molecule, trimethylamine-*n*-oxide (TMAO).[8−14]

TMAO belongs to a class of small organic molecules (osmolytes) present in organisms living under conditions of water stress, and it primarily acts as a regulator of the osmotic pressure in intracellular fluids.[15,16] Osmolytes, in contrast to monohydric alcohols,[17] typically stabilize the native state of globular proteins against thermal denaturation.[18] In this respect, TBA and TMAO exhibit very different effects on protein folding and other protein processes. In particular, TMAO counteracts the denaturing effects of urea[19−21] and, like a chemical chaperone, induces the renaturation of proteins.[22,23] Both TMAO[18] and TBA,[17] at least at low concentrations, do not directly interact with proteins. Therefore, their antithetic action on biosolutes must be correlated to differences in their respective hydration properties and/or in their association behavior.

One fundamental and recurring hypothesis is that solutes act on protein stability by altering water structure.[24] Recently, this hypothesis has been tested by applying thermodynamic analysis to calorimetric data on aqueous solutions of protein stabilizers and denaturants.[24] Contrary to widely held expectations, the data showed that there is no direct correlation between a solute's effect on water structure and its effect on protein stability. Likewise, a recent theoretical study of the interaction of denaturing and nondenaturing solutes with water by several computational methods showed that there is no a clear difference in the effect on water structure between urea and TMAO.[25] These results indicate that efforts to explain TBA and TMAO's opposite effects on protein stability should focus on other hypotheses instead of their effect on water structure.

In our recent research, we have focused on this pair of solutes to understand the molecular and thermodynamic basis of the effect of these solutes on biopolymer processes.[8−10] According to molecular dynamics simulations,[11,12] the experimental data show that the TMAO molecules tend to stabilize highly ordered, noninteracting hydration structures and do not show any self-aggregation behavior. In this case, a diffuse solute−solvent intermixing persists up to the highest solute concentration. In contrast, TBA perturbs the water's structure less, but its hydration shells strongly overlap and, at intermediate alcohol concentrations, the solute molecules show marked self-association.[7] As a consequence, the corresponding hydration number turns out to be strongly dependent on alcohol concentration.[10] Actually, solvent-induced interactions, such as the hydrophobic interactions, can be viewed as the result of hydration shells overlapping. These interactions can be expressed as the derivative of the solvent-induced part of the free energy with respect to the solute−solute distance; if the perturbations caused by distinct solute molecules do not overlap, then there is no reason to expect some dependence of the free energy upon solute−solute distance, that is, the existence of solvent-induced interactions.[15] On the basis of the above ideas, we previously suggested that small amounts of alcohol affect molecular processes, such as protein folding or surfactant micellization, by modulating the hydrophobic effect, and that this phenomenon is related to the X_2 dependence of the cosolute hydration number.[10] According to the Shinoda point of view[1] and the Privalov analysis of the protein structures done on a thermodynamic bases,[2] our studies indicate that the hydrophobic interaction at low concentrations of hydrophobic groups is repulsive and disfavors the aggregation of nonpolar species. Therefore, the attenuation of hydrophobic effects, at low alcohol concentrations, should favor the clustering of hydrophobic groups, stabilizing more compact protein structures. Larger amounts of alcohol will favor direct interactions between hydrophobic side chains and alcohol molecules, leading to less compact protein molecules and finally to unfolding. For TMAO molecules, the hydration number is almost independent of X_2, and only minor attenuation of the hydrophobic effect is expected.[26]

Although the influence of TBA or TMAO on protein folding is well-known in the literature, new insight must be achieved to understand their microscopical mechanism. In the present work, to further clarify the factor largely responsible for the effects of alcohols or osmolytes on protein folding, we choose to explore the hydration properties and self-association behavior of another common osmolyte, glycine betaine (GB). GB can be regarded as a tetramethylammonium ion in which one of methyl protons has been replaced by a carboxylate group. GB is one of the most effective osmolytes in stabilizing protein and membrane structure.[27−30] An important effort to characterize the hydration properties of TMAO and GB comes from a series of recent molecular dynamics simulation studies.[11,12] The general picture emerging from this series of molecular dynamics simulations is that a diffuse intermixing of water and solute occurs even at the highest solute concentrations close to the TMAO or GB solubility limit at room temperature. This agrees with our data on aqueous solutions of TMAO.[8−10] It is important to add new experimental evidence and to extend the study to aqueous solutions of other osmolytes.

Following the results of our previous work, we report here a Raman spectroscopy study of the hydration properties and self-association behavior of TBA, TMAO, and GB in aqueous solutions as a function of the mole fraction X_2 in the water-rich region of composition ($0 < X_2 < 0.06$). Raman scattering studies of water in the presence and absence of solute can, in principle, provide information on the perturbation on water structure by the introduced solutes. On the other hand, the analysis of the shift in the C−H stretching bands can provide information on the self-aggregation of solutes as a function of concentration. The properties of the aqueous solutions of TBA, TMAO, and GB were also studied by density and compressibility measurements, which give information on the overall behavior of the mixture.

To establish the existence of a correlation between the effects of these three solutes on the micellization process and changes in the properties of the solvent, the behavior of the critical micelle concentration (cmc) of sodium dodecyl sulfate (SDS) was also investigated as a function of the added amount of TBA, TMAO, and GB. The aim of this work is to present further evidence in support of the hypothesis that the effect of small solutes (alcohols and osmolytes) on micelle or protein stability can be related to the nonadditivity perturbations of the H-bonded network of the solvent water caused by the solutes, and that the aggregation of alcohol molecules is an important factor enhancing the effect of alcohol.

Experimental Section

All samples were prepared by weight, and by using bidistilled and deionized water. TBA alcohol (Aldrich product), anhydrous TMAO (Aldrich product), GB (Aldrich product) and SDS (Aldrich product) were used without any further purification.

Raman spectra were recorded exciting with the 514.5 nm radiation of an Innova 90 Coherent argon ion laser. The scattered light in a 90° scattering geometry was dispersed by a U1000 Isa Jobin-Yvon double monochromator equipped with holographic gratings. The detector was constituted by an electrically cooled (−30°C) Hamamatsu photomultiplier. The polarized Raman spectra (in the usual vertical-vertical VV configuration) were recorded in the 2600−4000 cm^{-1} region with a spectral resolution of 2 cm^{-1}. Separate spectra of the CH stretching region 2600−3200 cm^{-1} were also measured with higher spectral resolution (1 cm^{-1}) in order to analyze with enough accuracy the frequency dependence of the bands. Standard fitting procedures were employed to evaluate spectral parameters. The employed method allowed for the observation of band position shifts larger than 0.5 cm^{-1}, as evaluated comparing independent measurements. The temperature of the sample was controlled using an Haake model F6 ultrathermostat with circulating water (accuracy of ±0.5 °C).

Conductivity measurements were performed by means of a conductometer, model CDM 83, from Radiometer, Copenhagen, on H_2O/SDS, H_2O/SDS/TBA, H_2O/SDS/TMAO, and H_2O/SDS/GB solutions. Measurements were performed at a temperature of 25 °C. The temperature was controlled, and the variation was 0.05 °C. The cmc values were determined at the break point of two nearly straight-lined portions of the specific conductivity versus surfactant concentration plots.

Ultrasonic velocities were measured at 25 °C on H_2O/TBA, H_2O/TMAO, and H_2O/GB samples by means of a sing-around velocimeter, model 6080, from Nusonic Corp., New Jersey. The temperature control was better than 0.1 °C, and the measurements of sound velocity were reproducible within 0.1 m s^{-1}. From the values of sound velocity, v_s, and density, ρ, the adiabatic compressibility, β_s, was calculated by means of the relation $\beta_s = 1/(v_s^2 \cdot \rho)$. The densities used to calculate β_s were taken from the literature for the H_2O/TBA solutions.[31] For H_2O/TMAO and H_2O/GB solutions, densities were measured using a densimeter Anton Paar DMA 512; the reproducibility of the data is better than $\pm 1 \times 10^{-4}$.

Results and Discussion

Effect of TBA, TMAO, and GB on the Micellization Process. In this section, we report the results obtained on the effect of TBA, TMAO, and GB molecules on a typical process governed by hydrophobic interactions, such as the micellization of a surfactant in aqueous solution. The behavior of the cmc of SDS was investigated as a function of added amounts of TBA, TMAO, or GB in the dilute range of concentrations ($0 < X_2 < 0.04$) by conductivity measurements. Figure 1 clearly shows that TBA affects the micellization process. The cmc value in the presence of TBA decreases at low alcohol mole fractions X_2 and increases at high X_2, passing through a minimum at $X_2^* = 0.025$ where the hydrophobic clustering of TBA molecules starts.[7] On the contrary, no variations in the cmc were observed upon adding TMAO, and only a small decrease was observed upon adding GB. Therefore, these two osmolytes substantially do not perturb the Gibbs energy of the micellization process. Upon folding, a protein buries its nonpolar amino acids into a core, away from contact with water. In this respect, the folding of a protein is similar to the micellization process. Actually, in the concentration range where the cmc and thus the free energy of micellization show a minimum, a maximum is observed for the transition enthalpy and entropy in the case of the thermal denaturation of a lysozyme in H_2O/TBA mixtures.[17] The data indicate that low alcohol concentrations ($X_2 < X_2^*$) favor the micellization process, and that the TBA hydrophobic clustering above the threshold concentration X_2^* plays a critical role in altering the folding of proteins and the micellization process. In contrast to TBA, both TMAO and GB do not affect the micellization process and do not perturb the Gibbs energy of stabilization of proteins near room temperature.[32] In other words, these osmolytes have almost no effect on the strength of the hydrophobic interactions. This permits high fidelity in folding the protein without greatly diminishing the driving force exerted through the hydrophobic effect.

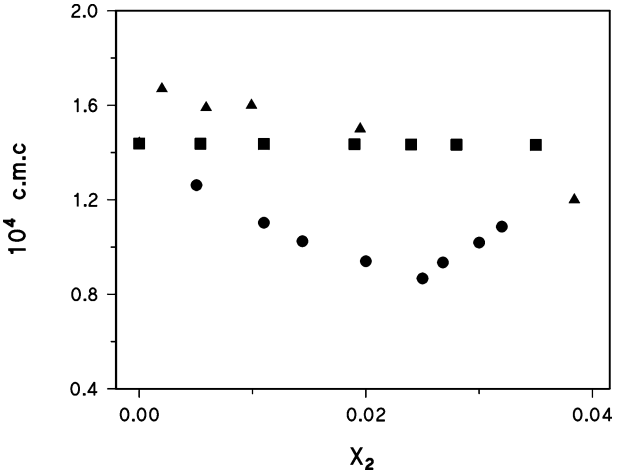

Figure 1. SDS cmc (expressed as a molar fraction) in (▲) H_2O/GB, (■) H_2O/TMAO, and (●) H_2O/TBA solutions as a function of the molar fraction X_2 of GB, TMAO, or TBA cosolutes.

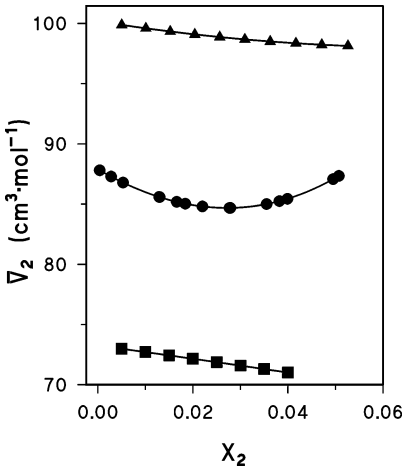

Figure 2. Partial molar volume $\bar{V}_2$ of (▲) GB, (■) TMAO, or (●) TBA in water solutions vs X_2. Lines are guides for the eye.

Volumetric Properties of H_2O/TBA, H_2O/TMAO, and H_2O/GB Aqueous Mixtures. The partial molar volumes $\bar{V}_2$ (Figure 2) of TBA, TMAO, and GB in aqueous solutions were evaluated from solution densities by the standard procedures indicated in the literature. For H_2O/TBA systems, $\bar{V}_2(X_2)$ passes through a minimum at $X_2^* = 0.027$, a value practically coincident with the X_2^* corresponding to the minimum in the cmc plot versus X_2 (Figure 1). For both TMAO/H_2O and GB/H_2O systems, the values of $\bar{V}_2(X_2)$ show an almost linear decrease with X_2 over the whole examined interval of molar fraction.

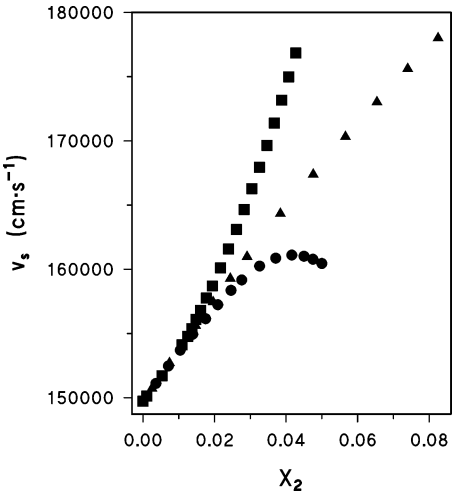

Figure 3. Ultrasonic velocity v_s in aqueous solutions of (▲) GB, (■) TMAO, (●) TBA vs X_2.

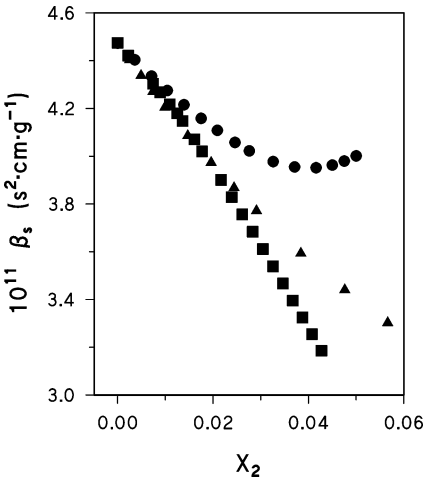

Figure 4. Adiabatic compressibility β_s of (▲) H_2O/GB, (■) H_2O/TMAO, and (●) H_2O/TBA samples vs X_2.

The decreasing trend of $\bar{V}_2(X_2)$ at low TBA concentrations ($X_2 < X_2^*$) can be explained in terms of a difference between the density of water belonging to the hydration shells and that of the bulk phase and considering the overlapping of the hydration layers as the TBA concentration increases.[33] For the H_2O/TBA solution at $X_2 > X_2^*$, previous IR and compressibility data indicate a transition from a system in which single hydrated TBA monomers predominate to a solution characterized by alcohol−alcohol interactions. From this description, it follows that, for $X_2 > X_2^*$, $\bar{V}_2(X_2)$ increases rapidly toward the $\bar{V}_2$value of the pure alcohol. The almost linear decrease of $\bar{V}_2(X_2)$ with X_2 for the TMAO and GB cases indicates, according to simulation data[11,12] and other suggestions in the literature,[8−10] a substantial absence of self-association of these two solutes as well as negligible overlapping of their hydration shells, at least in the concentration range examined.

Compressibility Measurements. The concentration dependence of the sound velocity v_s in aqueous solutions of monohydric alcohols exhibits some well-known singularities. In particular, in H_2O/TBA samples, v_s shows a pronounced maximum at $X_2^* = 0.04$ (Figure 3), whereas the adiabatic compressibility $\beta_s = 1/(v_s^2\rho)$ passes through a minimum at the same X_2 (Figure 4). This behavior can be explained by the formation of fairly incompressible H_2O/TBA units at low alcohol concentrations. Upon increasing the alcohol concentration, the rate of association between alcohol molecules progressively

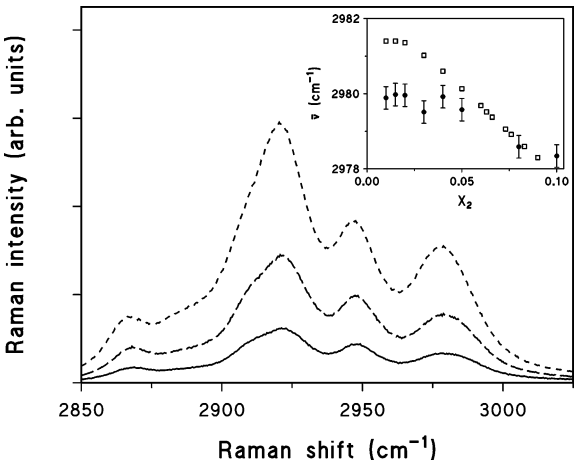

Figure 5. Raman spectra in the C−H stretching region of H_2O/TBA solutions (25 °C) at selected values of solute molar fraction X_2: (—) $X_2 = 0.02$; (− − −) $X_2 = 0.04$; and (- - -) $X_2 = 0.08$. Inset: X_2 dependence of the frequency position of the IR (□) and Raman (●) high-frequency band.

grows, accompanied by the formation of more compressible clusters of TBA molecules. For both the TMAO and GB aqueous solutions, the values of v_s and β_s (Figures 3 and 4) at low X_2 values are coincident with that of the H_2O/TBA system, thus indicating again the formation of incompressible solute−water entities. However, in these solutions, both v_s and β_s show almost linear trends in the overall concentration range investigated, indicating the absence of molecular aggregation and of hydration shells overlapping.

With X_2 increasing, the β_s value for the TMAO/water system decreases at higher rates when compared to the GB/water one, which remains sensibly more compressible at higher solute concentrations. This situation may be related to the different properties of the hydration sphere for the two solutes and is consistent with their different effect on the water HB network, as evidenced by the OH Raman spectra that will be discussed below.

Raman Data: The C−H Stretching Bands. The micelle formation is accompanied by large shifts (4−8 cm^{-1}) in the fundamental frequencies of the symmetric and antisymmetric alkyl stretching bands.[34−37] Similar effects were also found in a previous IR absorption study on the association of monohydric alcohols in water[38] and are here confirmed by the analysis of Raman spectra in the C−H stretching region. Figure 5 shows the Raman spectra, at $T = 25$ °C, in the C−H stretching region of TBA in water at $X_2 = 0.02$, 0.04, and 0.08. From this figure, the concentration dependence of the C−H stretching frequencies is evident. According to IR absorption data, below $X_2^* = 0.025$, the frequencies and shapes of all Raman bands are constant, and shifts of the bands to lower frequencies are observed for $X_2 > X_2^*$ (see inset to Figure 5). The observed trend is consistent with the description of the self-association of TBA molecules inferred from density and compressibility data. The high C−H stretching frequencies in the $0-X_2^*$ concentration range can be attributed to the aqueous local environment of the $-CH_3$ groups. For $X_2 > X_2^*$, the frequency changes as a function of X_2 toward the values typical of pure alcohol. This behavior indicates an increasing amount of hydrophobic clustering of TBA molecules as the concentration is increased. In both TMAO (Figure 6) and GB (Figure 7) solutions, no shift of the C−H stretching band is observed. For these two solutes, the C−H stretching bands maintain the characteristic features of a monomeric dispersion of solute in

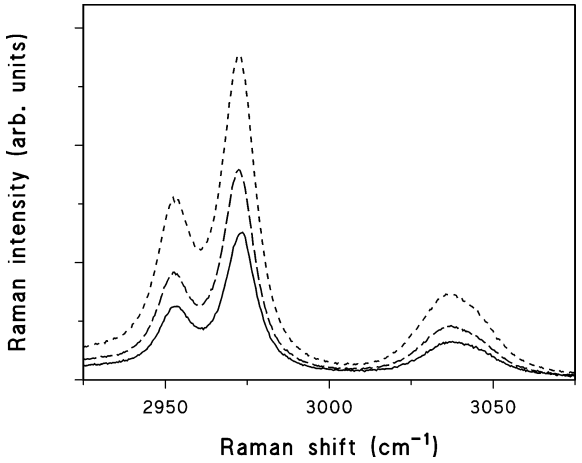

Figure 6. Raman spectra in the C−H stretching region of H_2O/TMAO solutions (25 °C) at selected values of solute molar fraction X_2: (—) $X_2 = 0.02$; (− − −) $X_2 = 0.04$; (- - -) $X_2 = 0.08$.

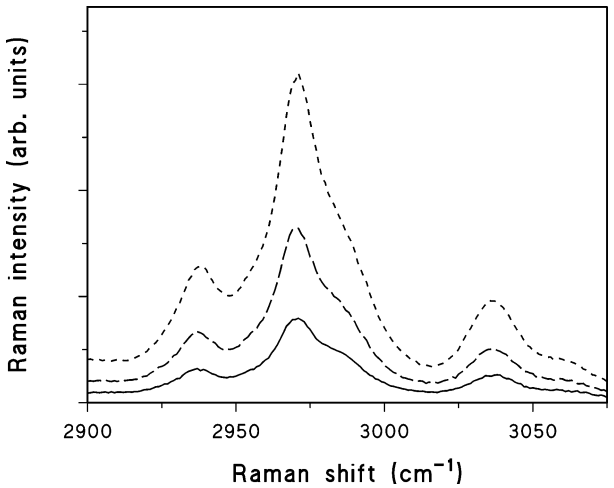

Figure 7. Raman spectra in the C−H stretching region of H_2O/GB solutions (25 °C) at selected values of solute molar fraction X_2: (—) $X_2 = 0.02$; (− − −) $X_2 = 0.04$; (- - -) $X_2 = 0.08$.

water in the overall concentration range, confirming the absence of hydrophobic clustering among solute molecules in the examined range of concentrations.

Recently, there was an interesting simulation study that attempted to explain why TBA aggregates in water while TMAO does not.[14] It is shown that the different behavior of these two solutes is almost entirely due to the fact that the average interaction of water with the hydrophilic end of TMAO (the oxygen) is much stronger than its interaction with that of TBA (the hydroxyl group). Accordingly, a recent work based on both NMR and molecular dynamics simulation data evidences that TMAO has a stronger hydrophilic character than TBA.[13] The methods employed allow for the elucidation of the properties of the solutions at a microscopic level. For TBA solutions, the hydration shell is found to have both low density and large spatial spread, such that, above a molar fraction of 0.03, the reduction of hydrophobic hydration drives the self-aggregation of the solute. This effect does not take place in TMAO solutions, where the hydration shell is more compact and stable, maintaining its structure over a wider range of solute concentrations.

Raman Data: The O−H Stretching Band. Raman spectra of neat water in the fundamental O−H stretching region obtained between 15 and 45 °C are shown in Figure 8a. The Raman profile evidences distinct signatures at ∼3200, 3400, and 3600 cm^{-1} associated with distinct spectral components. The high-

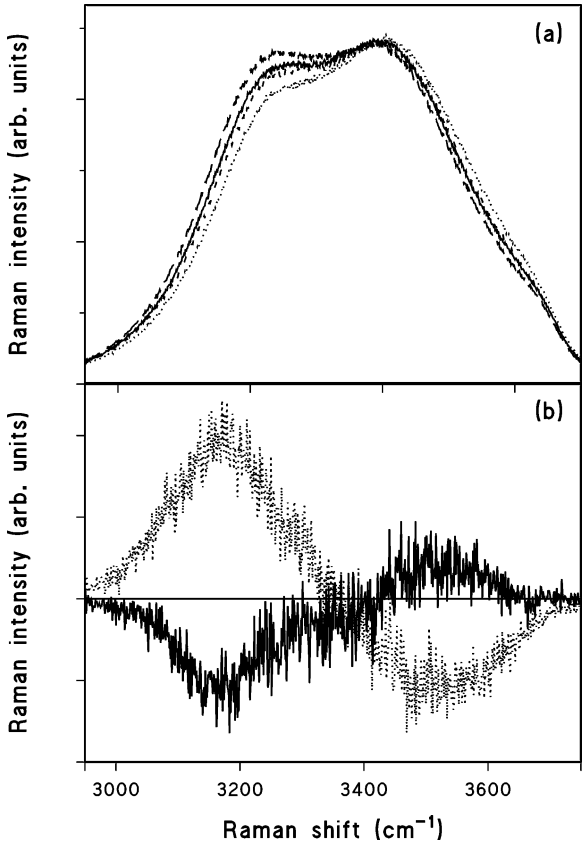

Figure 8. (a) Raman spectra of the OH stretching band of neat water at different temperatures (15, 25, 35, and 45 °C). The intensity decreases at low frequencies and increases at high frequencies with increasing temperature. (b) Raman difference spectra obtained by subtracting the reference spectrum measured at 25 °C from the spectra obtained at 35 °C (—) and 15 °C (•••).

frequency shoulder is related to OH oscillators of water molecules not participating, as proton donors, in the formation of hydrogen bonds.[39−41] The two principal components are mainly due to water molecules fully embedded in H-bonded structures. More specifically, the lowest frequency component is assigned to a collective symmetric stretching mode in which O−H oscillators of the nearest molecules oscillate all in-phase.[39,41,42] This mode originates from ordered environments characterized by the tetrahedral ice-like arrangement. The intermediate component is attributed to water molecules in less symmetric structures where hydrogen bonds are partially elongated and distorted and the interoscillator phase correlations are lost.

The spectra measured at different temperatures have been scaled taking into account the reported weak dependence of the band intensity.[43] In this way, a quasi-isosbestic point is individuated around 3400 cm^{-1}, in agreement with the results directly obtained by absolute Raman measurements.[44] The effect of the temperature is better visualized by the difference spectra of Figure 8b calculated by subtracting the normalized water spectrum at 25 °C from the spectra of water at the selected temperatures. From Figure 8b, it is evident that the integrated intensity loss/gain below 3400 cm^{-1} upon temperature raise/decrease is accompanied by an intensity gain/loss in the integrated intensity above 3400 cm^{-1}. This fact indicates that OH oscillators at higher frequencies are replaced by OH oscillators at lower frequencies by lowering the temperature.[40] In part a of Figures 9, 10, and 11, the OH stretching band for H_2O/TBA, H_2O/TMAO, and H_2O/GB samples, respectively, at a solute mole fraction of $X_2 = 0.045$ and at a fixed temperature

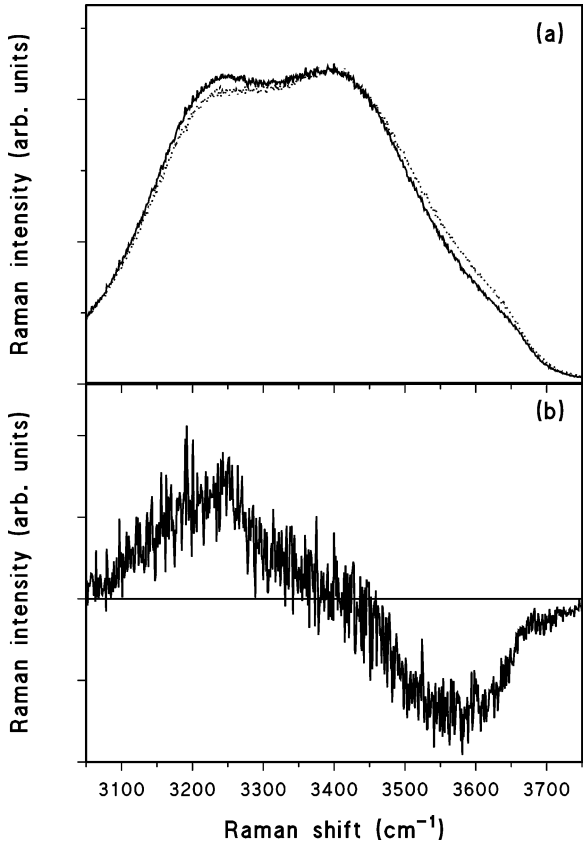

Figure 9. (a) Raman spectra of the OH stretching band in neat water (···) and in H_2O/TBA solution at $X_2 = 0.045$ (—) at 25 °C. (b) Difference spectrum obtained by subtracting the spectrum of pure water from that of the H_2O/TBA solution.

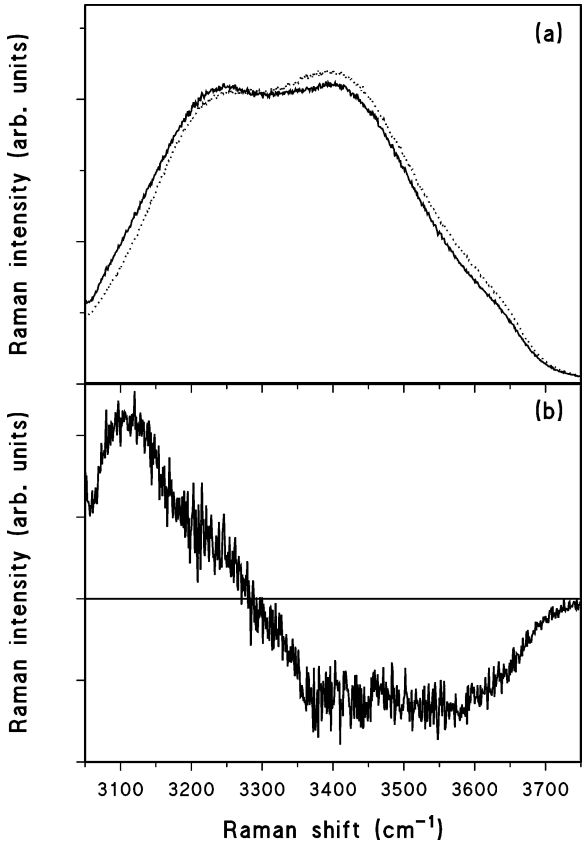

Figure 10. (a) Raman spectra of the OH stretching band in neat water (···) and in H_2O/TMAO solution at $X_2 = 0.045$ (—) at 25 °C. (b) Difference spectrum obtained by subtracting the spectrum of pure water from that of the H_2O/TMAO solution.

of 25 °C, are shown and compared with the spectrum of pure H_2O. The corresponding difference spectra obtained by subtracting the pure water spectrum from the spectra of the mixtures are also shown in the part b of the same Figures. The changes observed with respect to the pure H_2O band are very small, indicating a distribution of hydrogen bond energies only slightly perturbed by the presence of the solutes. It is evident from Figure 9 that TBA perturbs the water structure in a similar way to that achieved by lowering the temperature on the neat liquid. This fact is consistent with numerous studies in which it has been evidenced that hydrophobic solutes, in particular TBA, affect the spectroscopic and dynamical properties of water, reproducing the same effect of a temperature decrease.[45−48] The perturbation induced by TMAO on the water structure appears qualitatively similar to that of TBA (Figure 10). In any case, even though both TMAO and TBA cause the transfer of OH oscillators from the highest to the lowest frequency region of the spectrum, the involved OH distributions are located at very different frequencies, as clearly evidenced by comparing the TMAO and TBA difference spectra. In TMAO, the positive peak is located at lower frequencies (see Figure 10b) relative to that in TBA, indicating that the redistribution is accompanied by the creation of stronger hydrogen bonds. These data indicate, in agreement with molecular dynamics simulation results and with previous IR absorption studies, that TMAO and TBA's interactions with water are different, and that water molecules are more tightly coordinated by TMAO than by TBA. This result is consistent with the relative strength of their dipole moment, being $\mu_{TMAO} \sim 3\mu_{TBA}$.

The effect of GB on the water structure appears to be qualitatively different. In fact, unlike TMAO and TBA, the changes caused by the addition of a small amount of GB (Figure 11) partly reproduce the effect of a temperature increase in pure water. This is evident observing the intensity decrease at the low frequency side of the difference spectra in Figure 11b related to ordered ice-like species. However, the addition of GB is also accompanied by a small intensity decrease of the highest frequency region, attributable to more weakly hydrogen-bonded species, indicating that the addition of GB reduces "free" OH oscillators.

The different effect of GB on the water structure is likely related to its zwitterionic nature. It is known that ionic and hydrophobic solutes exert a different perturbation effect on the water organization.[49] More precisely, it is expected that ionic and polar groups act disturbing the ordered network of water, whereas hydrophobic moieties contribute to the enhancement of the ice-like H-bonding environments. In this sense, the experimental data suggest that, for GB, the restructuring effect, as a result of the hydrophobic portions of the molecule, is partially reduced because of the opposite action exerted by the presence of net charges. In this sense, it can be deduced that the disturbing effect of the ionic carboxylate group on the ice-like water is prevalent with respect to the structuring effect due to hydrophobic hydration.

Walrafen[39,44] reproduced the OH Raman band of liquid water using four Gaussian functional forms: two lower frequency components associated with the water molecules completely involved in the formation of four H-bonds (HB) and two higher frequency components related to water molecules not fully tetra coordinated (NHB). Several studies have confirmed the suitability of this deconvolution scheme.[50−52] In the present work, we used a simplified fitting procedure by employing only three components.[41] The adopted method, reproducing the experi-

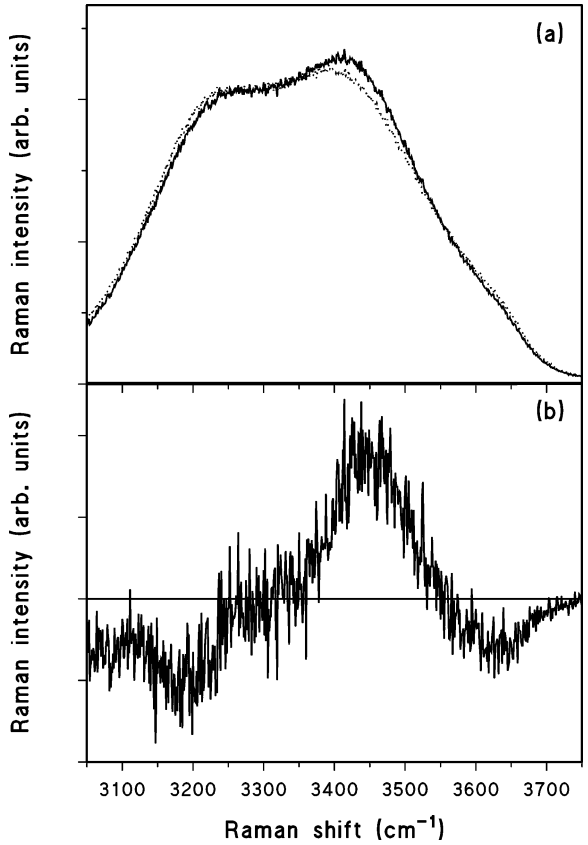

Figure 11. (a) Raman spectra of the OH stretching band in neat water (···) and in H_2O/GB solution $X_2 = 0.045$ (—) at 25 °C. (b) Difference spectrum obtained by subtracting the spectrum of pure water from that of the H_2O/GB solution.

mental data with a reduced number of parameters, is more convenient for comparison purposes. The polarized (VV) Raman profile has been decomposed using a 57% Gaussian/43% Lorentzian component (OH_1 at ∼3200 cm^{-1}) and two higher frequency Gaussian functions (OH_2 and OH_3 at ∼3400 and 3600 cm^{-1}). In any case, the width of the component has been constrained during the minimization procedure to the value obtained in pure water at 25 °C. An example of a fitting result is reported in Figure 12a for the Raman spectrum of pure water at 25 °C; such a deconvolution scheme closely resembles the one recently employed by Matsuura and co-workers.[53,54] In terms of structural properties of the liquid system, the three components can be directly related to the three classes of oscillators discussed above. In particular, the low-frequency component OH_1 is assigned to the collective in-phase OH-stretching mode of ordered and tetrahedrally coordinated water molecules. On the contrary, the high-frequency bands of OH_2 and OH_3 may be referred to water molecules in which the H-bonds are distorted or broken to some extent. In particular, OH_3 gives only a minor contribution (about 3−4%) to the total stretching band and is manly assigned to "free" OH oscillators of water molecules. The temperature decreasing strongly affects the relative intensity of the components (A_1, A_2, and A_3), causing an overall intensity redistribution toward the low-frequency component. More precisely, lowering the temperature from 75 to 10 °C causes the increase in A_1 (from 37% to 48%) and the concomitant decrease in A_2 (from 58% to 48%) and A_3 (from ∼4.5% to ∼3.3%). This reflects the enhancement of hydrogen bonding at lower temperatures, which give rise to patches of tetrahedrally bonded water molecules. The intensity changes can also be easily quantified within the 35−15 °C temperature range, where the magnitude of the spectral variations is comparable

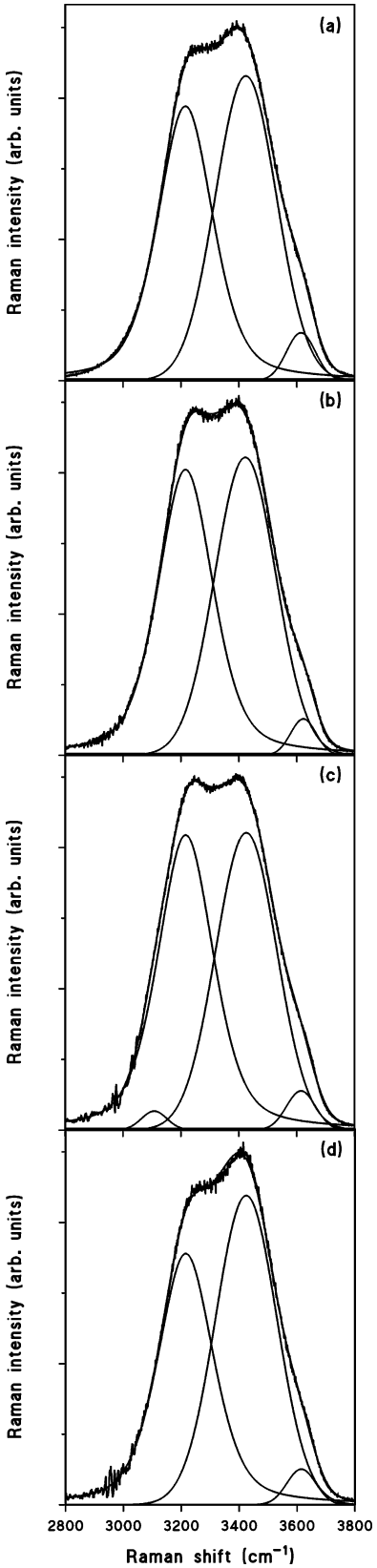

Figure 12. Raman spectra in the OH stretching region in neat water (a), H_2O/TBA (b), H_2O/TMAO (c), and H_2O/GB (d) solutions; $X_2 = 0.045$, $T = 25$ °C. The different spectral components obtained by a fitting procedure are also shown.

to that induced by the solutes (see Figures 8−11 and Table 1). In light of this approach, the ratio $R = A_1/A_2$ can provide information about the fraction of water in the system that takes part in the regular tetrahedral structure with strong H-bonds. R

TABLE 1: Intensity Percentages (%A_i) Relative to the Spectral Components of Figure 12

	X_i	T (°C)	%A_1	%A_2	%A_3	%A_{W-S}	R^a
water	1	15	47.9	48.7	3.4		0.98
water	1	25	46.2	50.1	3.7		0.90
water	1	35	44.9	51.3	3.7		0.87
TBA	0.045	25	48.5	49.0	2.5		0.99
TMAO	0.045	25	48.7	47.1	2.9	1.3	1.03
GB	0.045	25	44.1	53.0	2.9		0.83
error			± 0.5	± 0.5	± 0.2	± 0.5	± 0.02

[a] R is the A_1/A_2 intensity ratio (see text for details).

changes from 0.87 to 0.98, decreasing the temperature from 35 to 15 °C (Table 1), in agreement with other reports.[53,54]

To provide a more quantitative description of the observed changes in Raman spectra of water in the presence of TBA, TMAO, and GB, we have applied the same interpretative scheme to describe the spectrum of water in these three systems. A first-order fitting procedure has been applied, including both the CH and OH stretching regions. Then, after the subtraction of the CH stretching, a refinement fitting procedure has been applied on the OH distribution. The frequency and width of the three components have been fixed to the values of pure water, and only the relative amplitude of the components is allowed to change during the minimization process; the resulting percent of the integrated areas is reported in Table 1.

This procedure is in line with a model of solute hydrophobic hydration that states that the differences between bulk water and hydration water arise from a varying ratio between the more ordered and less ordered H-bonding environments.[24] The three-component fit reproduces with good accuracy the spectrum of water of TBA/H_2O, indicating that only minor contributions arise from alcoholic OH modes. As it can be seen from Figure 12b and from the data of Table 1, the OH distribution in the TBA/H_2O solution at 25 °C is similar to the spectrum of neat water at 15 °C.

This comparison is especially true for the A_1/A_2 ratio and reproduces the situation depicted by the difference spectra at low frequencies. In this respect, it seems that the addiction of TBA at $X_2 = 0.045$ induces the formation of ordered patches of water molecules, analogous to that originated by lowering the temperature of the neat sample by 10 °C. This is in agreement with the changes in several chemical-physics properties observed in the presence of TBA.[45−49]

The three-component fit cannot adequately reproduce the OH stretching Raman band of water in the presence of TMAO; in fact there is an evident failure of the fit located in the low-frequency region. To adequately reproduce the band, we need to introduce an additional weak Gaussian component centered at about 3100 cm^{-1}. In Figure 12c, the experimental OH stretching band is reported for the TMAO/H_2O sample at $X_2 = 0.045$ together with the calculated curve decomposition; the fitted curve is virtually indistinguishable from the measured one. This situation is in perfect agreement with the conclusion gained by an analogous IR study on the OH stretching band.[8] Here, the low frequency component has been assigned to the two water molecules tightly bound to the N−O group of the TMAO, that is, to the H_2O−TMAO OH− O bonds, which are stronger than the mean water−water hydrogen bonds. These results indicate that no interactions exist in pure water, in the temperature range considered, that influence the OH stretching frequency in the same way as the interaction between TMAO and water. In any case, the TMAO explicates a clear structuring action, enhancing the collective component at 3200 cm^{-1} (see Table 1). In practice, both the fitting results and the analysis of the difference spectra seem to indicate that adding TMAO leads to the formation of stronger hydrogen bonds within the system, either due to the specific TMAO−H_2O interactions or due to the hydrophobic hydration phenomenon. This is likely in line with the low compressibility of the TMAO/water system at high X_2 and with the simulation results of Paul and Patey.[14]

Like the TBA/water solutions, the three-component fit reproduces with good accuracy the spectrum of water of the GB/water solutions. As shown in Figure 12d and Table 1, the fitting results on the GB/water system evidence that the main effect of GB is the enhancement of the central component, due to distorted hydrogen bonds. The population of such species also grows at the expense of the more ordered oscillators involved in stronger H-bonds. This is in agreement with the observations made using the difference spectra and confirms the destructuring properties of GB, in contrast with the conclusion gained for TBA and TMAO.

Table 1 indicates that, for all three solutes, there is a decrease in the intensity of the highest frequency component OH_3 assigned to free OH oscillators. This is probably due to the formation of new H-bonds between the H_2O molecules and the hydrophilic group of these solutes. On the whole, these data show that there is no direct correlation between a solute's effect on the water structure and its effect on micelle or protein stability.

Conclusions

Raman scattering spectra of water in the presence of TBA, TMAO, or GB provide a coherent description of the water structure perturbations induced by these three solutes: spectral data indicate that adding both TBA and TMAO induces the formation of ordered patches of water molecules analogous to that originated by lowering the temperature of neat liquid water. Unlike TMAO and TBA, the changes caused by the addition of a small amount of GB partly reproduce the effect of a temperature increase in pure water. On the whole, these data show that there is no direct correlation between a solute's effect on the water structure and its effect on micelle or protein stability. Thus, a solute's effect on water structure is not the determining factor in its effect on micelle or protein stability. Results indicate that, while TBA starts to self-aggregate at approximately $X_2^* = 0.025$, both TMAO and GB do not exhibit any significant self-aggregation up to the highest concentration considered. Moreover, nonadditive perturbations of the H-bonded networks of solvent water are observed in the case of TBA solutions, but are absent in both the TMAO and GB cases. These data further support our suggestions that the origin of the solvent-mediated interactions is in the nonadditivity of the effects of the solute perturbations on the H-bond network in the solvent water, and that the absence of these nonlinear effects in TMAO and GB water solutions allow tracing of the microscopical mechanism of the neutrality of these osmolytes toward hydrophobic effects. This confers the compatibility to these two osmolytes, which can be accumulated at high concentration without interfering with biochemical processes in the cell.

References and Notes

(1) Shinoda, K. *J. Phys. Chem.* **1977**, *81*, 1300.

(2) Privalov, P. L. *Biochem. Mol. Biol.* **1990**, *25*, 281.

(3) Southal, K. A.; Dill, K. A.; Haymet, A. D. J. *J. Phys. Chem. B* **2002**, *106*, 521.

(4) Eagland, D. In *Water: A Comprehensive Treatise*; Franks, F., Ed.; Plenum: New York, 1975; Vol. 4, pp 305−518.

(5) Blandamer, M. J. In *Advances in Physical Organic Chemistry*; Gold, V., Ed.; Academic Press: New York, 1977; Vol. 14, pp 203−351.
(6) Kresheck, G. C. In *Water: A Comprehensive Treatise*; Franks, F., Ed.; Plenum: New York, 1975; Vol. 4, pp 95−167.
(7) Onori, G.; Santucci, A. *J. Mol. Liquids* **1996**, *69*, 161 and references therein.
(8) Freda, M.; Onori, G.; Santucci, A. *J. Phys. Chem. B* **2001**, *105*, 12714.
(9) Freda, M.; Onori, G.; Santucci, A. *Phys. Chem. Chem. Phys.* **2002**, *4*, 4979.
(10) Di Michele, A.; Freda, M.; Onori, G.; Santucci, A. *J. Phys. Chem. A* **2004**, *108*, 6145.
(11) Noto, R.; Martorana, V.; Emanuele, A.; Fornili, S. L. *J. Chem. Soc., Faraday Trans.* **1995**, *91*, 3803.
(12) Fornili, A.; Civera, M.; Sironi, M.; Fornili, S. L. *Phys. Chem. Chem. Phys.* **2003**, *5*, 4905.
(13) Sinibaldi, R.; Casieri, C.; Melchionna, S.; Onori, G.; Segre, A. L.; Viel, S.; Mannina, L.; De Luca, F. *J. Phys. Chem. B* **2006**, *110*, 8885.
(14) Paul, S.; Patey, G. N. *J. Phys. Chem. B* **2006**, *110*, 10514.
(15) Yancey, P. H.; Clark, M. E.; Hand, S. C.; Bowlus, R. D.; Somero, G. N. *Science* **1982**, *217*, 1214.
(16) Somero, G. N. In *Water and Life*; Somero, G. N., Osmond, C. B., Bolis, C. L., Eds.; Spinger-Verlag: Berlin, 1992; p 3.
(17) Cinelli, S.; Onori, G.; Santucci, A. *J. Phys. Chem. B* **1997**, *101*, 8029.
(18) Arakawa, T.; Timasheff, S. N. *Biophys. J.* **1985**, *47*, 411.
(19) Yancey, P. H.; Somero, G. N. *Biochem. J.* **1979**, *183*, 317.
(20) Liu, T. Y.; Timasheff, S. N. *Biochemistry* **1994**, *33*, 12695.
(21) Lever, M.; Randall, K.; Galinski, E. A. *Biochim. Biophys. Acta* **2001**, *135*, 1528.
(22) Baskakov, I.; Bolen, D. W. *J. Biol. Chem.* **1998**, *273*, 4831.
(23) Baskakov, I.; Kumar, R.; Srinivasan, G.; Ji, Y.; Bolen, D. W.; Thompson, E. B. *J. Biol. Chem.* **1999**, *274*, 10693.
(24) Batchelor, J. D.; Olteanu, A.; Tripathy, A.; Pielak, G. J. *J. Am. Chem. Soc.* **2004**, *126*, 1958.
(25) Maclagan, R. G. A.; Malardier-Jugroot, C.; Whitehead, M. A.; Lever, M. *J. Phys. Chem. A* **2004**, *108*, 2514.
(26) Bulone, D.; San Biagio, P. L.; Palma-Vittorelli, M. B.; Palma M. U. *Nuovo Cimento Soc. Ital. Fis.* **1993**, *15D*, 443.
(27) Papageorgiu, G. C.; Murata, N. *Photosynth. Res.* **1995**, *44*, 243.
(28) Goeller, K.; Galinski, E. A. *J. Mol. Catal. B: Enzymol.* **1999**, *7*, 37.
(29) Di Domenico, R.; Lavacchia, R. *Biochem. Eng.* **2002**, *10*, 27.
(30) Jolivet, Y.; Lahrer, F.; Hamelin, J. *Plant Sci. Lett.* **1982**, *25*, 193.
(31) Brunel, R. F.; Van Bibber K. *International Critical Tables*; McGraw Hill: New York, 1933.
(32) Anjum, F.; Rishi, V.; Ahmad, F. *Biochim. Biophys. Acta* **2000**, *75*, 1476.
(33) Calandrini, V.; Fioretto, D.; Onori, G.; Santucci, A. *Chem. Phys. Lett.* **2000**, *324*, 344.
(34) Umemura, J. H.; Cameron, D. G.; Mantsch, H. H. *J. Am. Chem. Soc.* **1980**, *84*, 2272.
(35) Umemura, J. H.; Mantsch, H. H.; Cameron, D. G. *J. Colloid Interface Sci.* **1981**, *83*, 558.
(36) Yang, P. W.; Mantsch, H. H. *J. Colloid Interface Sci.* **1986**, *113*, 218.
(37) Cross, W. M.; Kellar, J. J.; Millar, J. D. *Appl. Spectrosc.* **1992**, *46*, 701.
(38) D'Angelo, M.; Onori, G.; Santucci, A. *J. Chem. Phys.* **1994**, *100*, 3107.
(39) Monosmith, W. B.; Walrafen, G. E. *J. Chem. Phys.* **1984**, *81*, 669.
(40) Walrafen, G. E.; Fisher, M. R.; Hokmabadi, M. S.; Yang, W. H. *J. Chem. Phys.* **1986**, *85*, 6970.
(41) Walrafen, G. E.; Chu, Y. C. *J. Phys. Chem.* **1995**, *99*, 11225.
(42) Geen, J. L.; Lacey, A. L.; Sceats, M. G: *J. Phys. Chem.* **1986**, *90*, 3958.
(43) Hare, D. E.; Sorensen, C. M. *J. Chem. Phys.* **1992**, *96*, 13.
(44) Walrafen, G. E.; Hokmabadi, M. S.; Yang, W. *J. Chem. Phys.* **1986**, *85*, 6964.
(45) Halfpap, B. L.; Sorensen, C. M. *J. Chem. Phys.* **1982**, *77*, 466.
(46) Sorensen, C. M. *J. Chem. Phys.* **1983**, *79*, 1455.
(47) Onori, G. *Chem. Phys. Lett.* **1989**, *154*, 212.
(48) Calandrini, V.; Deriu, A.; Onori, G.; Lechner, R. E.; Pieper, J. *J. Chem. Phys.* **2004**, *120*, 4759.
(49) Maeda, Y.; Kitano, H. *Spectrochim. Acta, Part A* **1995**, *51*, 2433.
(50) Carey, D. D. M.; Korenowsky, G. M. *J. Chem. Phys.* **1998**, *108*, 2669.
(51) Walrafen, G. E. *J. Chem. Phys.* **2004**, *120*, 4868.
(52) Sassi, P.; Paolantoni, M.; Cataliotti, R. S.; Palombo, F.; Morresi, A. *J. Phys. Chem. B* **2004**, *108*, 19557.
(53) Marinov, V. S.; Nickkolov, Z. R.; Matsuura, H. *J. Phys. Chem. B* **2001**, *105*, 9953.
(54) Marinov, V. S.; Matsuura, H. *J. Mol. Struct.* **2002**, *610*, 105.